The Plant Cell, Vol. 20: 3359–3373, December 2008, www.plantcell.org

ASYMMETRIC LEAVES2-LIKE19/LATERAL ORGAN BOUNDARIES DOMAIN30 and *ASL20/LBD18* Regulate Tracheary Element Differentiation in *Arabidopsis* [W]

Takashi Soyano,[a,1] Siripong Thitamadee,[a,2] Yasunori Machida,[b] and Nam-Hai Chua[a,3]

[a] Laboratory of Plant Molecular Biology, The Rockefeller University, New York, New York 10065
[b] Division of Biological Science, Graduate School of Science, Nagoya University, Furo-cho, Chikusa-ku, Nagoya 464-8602, Japan

ASYMMETRIC LEAVES2 (AS2)/LATERAL ORGAN BOUNDARIES DOMAIN (LBD) family proteins are plant-specific nuclear proteins, and genes encoding several family members have been implicated in plant development. We investigated the function of two members of the *Arabidopsis thaliana AS2/LBD* family, *AS2-LIKE19* (*ASL19*)/*LBD30* and *ASL20/LBD18*, which encode homologous proteins. Both *ASL19* and *ASL20* were expressed in immature tracheary elements (TEs), and the expression was dependent on VASCULAR-RELATED NAC-DOMAIN PROTEIN6 (VND6) and VND7, which are transcription factors required for TE differentiation. Overexpression of *ASL19* and *ASL20* induced transdifferentiation of cells from nonvascular tissues into TE-like cells, similar to those induced upon *VND6/7* overexpression. By contrast, aberrant TEs were formed when a cDNA encoding a fusion protein of ASL20 with an artificial repressor domain (ASL20-SRDX) was expressed from its native promoter. These results provide evidence that ASL proteins positively regulate TE differentiation. In transgenic plants overexpressing both *ASL19* and *ASL20*, the xylem-deficient phenotype caused by the expression of dominant-negative versions of VND6/7 proteins was not rescued. However, ectopic expression of *VND7* was detected in plants overexpressing *ASL20*. Moreover, *VND* genes and their downstream targets were downregulated in ASL20-SRDX plants. Therefore, *ASL20* appears to be involved in a positive feedback loop for *VND7* expression that regulates TE differentiation-related genes.

INTRODUCTION

Arabidopsis thaliana ASYMMETRIC LEAVES2/LATERAL ORGAN BOUNDARIES DOMAIN6 (*AS2/LBD6*) and *LATERAL ORGAN BOUNDARIES/AS2-LIKE4* (*LOB/ASL4*) genes were first discovered as genes encoding members of the AS2/LBD protein family (Iwakawa et al., 2002; Shuai et al., 2002). Whole genome sequence information revealed that there are 42 genes predicted to encode the AS2/LBD family proteins in *Arabidopsis* (Iwakawa et al., 2002; Shuai et al., 2002). Results obtained by forward and reverse genetics indicate that several members of the AS2/LBD protein family play important roles in regulating various aspects of plant development, such as determination of stem cell fate (Bortiri et al., 2006), development of the embryo sac (Evans, 2007), leaf development (Ori et al., 2000; Semiarti et al., 2001; Xu et al., 2003), and lateral root formation (Inukai et al., 2005; Liu et al., 2005; Okushima et al., 2007; Taramino et al., 2007). Based on its expression pattern, the *LOB/ASL4* gene has been postulated to function in fate determination of a boundary between the initiating organ primordia and the stem cells from which they are generated (Shuai et al., 2002).

The AS2/LBD family of proteins are characterized by an N-terminal conserved domain with a $CX_2CX_6CX_3C$ motif and a Leu zipper–like sequence named the AS2/LOB domain. The AS2/LBD proteins likely execute their function in the nucleus, as the AS2/LBD–green fluorescent protein (GFP) fusion proteins localize to the nucleus (Iwakawa et al., 2002; Inukai et al., 2005; Naito et al., 2007). Consistent with this notion, the AS2/LOB domain of LOB protein was shown to bind to DNA in vitro (Husbands et al., 2007). The AS2 protein bound to sites in the promoter regions of the *KNAT1* (for *Knotted-like from Arabidopsis thaliana1*) and *KNAT2* genes, together with the AS1 protein (Guo et al., 2008), which also interacts with AS2 in vitro (Xu et al., 2003). *KNAT1* is expressed in the peripheral zone of the shoot apical meristem (Lincoln et al., 1994). *AS1* and *AS2* are required for the maintenance of *KNAT1* repression in developing leaves, once *KNAT1* expression is repressed at the start of the formation of the leaf primordium (Ori et al., 2000; Semiarti et al., 2001; Lin et al., 2003). The AS1-AS2 complex binding sites in the *KNAT1* promoter were found to be involved in *KNAT1* repression in developing leaves (Guo et al., 2008). Thus, the AS2/LBD family of proteins seem to regulate gene expression by interacting with specific DNA

[1] Current address: National Institute of Agrobiological Sciences, Kannon-dai, Tsukuba, Ibaraki 305-8602, Japan.
[2] Current address: Nara Institute of Science and Technology, Graduate School of Biological Sciences, Takayama 8916-5, Ikoma, Nara 630-0101, Japan.
[3] Address correspondence to chua@mail.rockefeller.edu.
The author responsible for distribution of materials integral to the findings presented in this article in accordance with the policy described in the Instructions for Author (www.plantcell.org) is: Nam-Hai Chua (chua@mail.rockefeller.edu).
[W] Online version contains Web-only data.
www.plantcell.org/cgi/doi/10.1105/tpc.108.061796

sequences, although the molecular mechanisms of the AS2/LBD family of proteins are still poorly understood.

Here, we report that two members of the *Arabidopsis* AS2/LBD protein family are involved in the differentiation of tracheary elements (TEs), the basic units that constitute xylem vessels. Xylem vessels are specialized tissues for the transport of water, nutrients, and signaling molecules and also provide plants with mechanical stability. TE precursors are differentiated from procambial and cambial cells, which are stem-like cells able to differentiate into other vasculature elements as well. During TE differentiation, a series of coordinated cellular events occurs, including changes in cytoskeletal organization, patterned cell wall deposition, and autolysis (Fukuda, 2004; Turner et al., 2007). The resulting mature TEs are distinguishable by their characteristic secondary cell walls with annular, spiral, reticulate, or pitted wall thickenings. Several factors, such as auxin, cytokinin, brassinosteroid (BR), xylogen, and the CLE family of peptides, have been implicated in the regulation of TE differentiation (Szekeres et al., 1996; Yamamoto et al., 1997; Choe et al., 1999; Caño-Delgado et al., 2004; Fukuda, 2004; Motose et al., 2004; Ito et al., 2006; Mähönen et al., 2006).

A gene expression analysis of *Arabidopsis* suspension culture cells identified two NAC (for Petunia NAM and *Arabidopsis* ATAF1, ATAF2, and CUC2)–domain transcription factors that function as positive regulators of TE differentiation: VASCULAR-RELATED NAC-DOMAIN PROTEIN6 (VND6) and VND7 (Kubo et al., 2005). Although Kubo et al. (2005) proposed that VND6 and VND7 act as transcription switches in the formation of metaxylem and protoxylem vessels, respectively, both being required for TE differentiation, Yamaguchi et al. (2008) recently reported that VND7 regulates not only the formation of protoxylem vessels in roots but also the formation of metaxylem vessels in roots and protoxylem vessels in the aerial parts of seedlings. Therefore, elucidating the regulation of VND6 and VND7 expression and determining their downstream gene networks are clearly important issues for understanding the molecular mechanisms underlying xylogenesis.

In this study, we investigated the function of *Arabidopsis* ASL19/LBD30 and ASL20/LBD18 (hereafter referred to as ASL19 and ASL20, respectively), two homologous AS2/LBD family proteins. Borghi et al. (2007) reported that embryogenesis of *jlo-1/asl19-1* mutants was arrested at the globular stage. However, *asl19-2* (a novel allele identified in this study) mutants did not show the embryonic phenotype (see Supplemental Figures 1A to 1E online). Furthermore, the phenotypic traits observed in *jlo-1* mutants were not suppressed when the recombinant *ASL19* cDNA that was fused to the *ASL19* promoter was introduced into the *jlo-1* mutant (see Supplemental Figure 1F online). These results suggest that the embryonic lethality is not linked to the *asl19* mutation. Our results showed that *ASL19* and *ASL20* were expressed in immature TEs. The expression was dependent on *VND6* and *VND7*. Moreover, overexpression of *ASL19* or *ASL20* induced transdifferentiation of cells from nonvascular tissues into TE-like cells, similar to those formed upon *VND6* and *VND7* overexpression. These results suggest that *ASL19* and *ASL20* regulate TE differentiation downstream of *VND6* and *VND7*. Further analyses showed that the generation of TE-like cells by *ASL19/20* overexpression required VND6 and VND7 activities and that *ASL20* overexpression induced ectopic expression of *VND7*. These results suggest that *ASL19* and *ASL20* are involved in a positive feedback loop that maintains or promotes *VND7* expression. We discuss the relationship between ASL19/20 and VND6/7 during TE differentiation.

RESULTS

Expression Profiles of *ASL19* and *ASL20*

Although there is a high level of sequence conservation in the AS2/LOB domain, the C-terminal regions of the AS2/LBD proteins are remarkably variable. ASL19 and ASL20 appear to be exceptions, because their C-terminal regions are 46.1% identical in amino acid sequences (Figure 1A). The similarity in the primary structures of these two proteins suggested that their function might be conserved in *Arabidopsis*. In addition, a database homology search uncovered two rice (*Oryza sativa*) AS2/LBD proteins (encoded by *Os03g14270* and *Os10g07510*) with C-terminal regions ~28 to 33.3% identical to those of ASL19 and ASL20 (Figure 1A). Homologies in the C-terminal regions of *Arabidopsis* and rice ASL19/20 counterparts suggested a conserved role of these proteins in the development of both monocots and dicots.

To understand the functions of ASL19 and ASL20, we generated *ProASL:EGFP* (*enhanced green fluorescent protein*)–*GUS* (β-*glucuronidase*) reporter constructs using a 2-kb sequence upstream of their corresponding coding sequences (see Methods) and analyzed their expression profiles in transgenic plants. Histochemical GUS staining was detected in the vascular tissues of hypocotyls, leaves, roots, developing floral organs, and siliques of transgenic plants (Figures 1B to 1J; see Supplemental Figure 2 online). GUS staining patterns in vasculatures were not distinguishable between the reporter constructs for *ASL19* and *ASL20*.

The *Arabidopsis* root has three or four files of metaxylem vessels surrounded by two files of protoxylem vessels in the vascular cylinder. Metaxylem vessels differentiate in the maturation zone of the root, whereas differentiation of protoxylem vessels occurs acropetally in the differentiation zone (Pyo et al., 2004). In the maturation zone of roots, strong GUS signals were detected in immature TEs of the outer two cell files of primary metaxylem vessels, although there was almost no staining in the central metaxylem vessels that differentiated later (Figures 1F and 1H). In the differentiation zone, expression of reporter genes was detected in immature TEs of the two cell files of protoxylem vessels but not in the cell files of metaxylem or other types of vascular cells (Figures 1G and 1I). The expression of the reporter genes was detected before the appearance of any obvious secondary cell wall thickening and lignin deposition (Figures 1F to 1J; compare with wall thickenings of mature TEs in Figure 2H or Figure 5I below), and GUS signals became stronger as the root developed. Similar patterns of *EGFP-GUS* expression in immature TEs were also observed in the expanding leaves (Figures 1C to 1E). In addition, GUS staining was detected around the quiescent centers of root tips (Figures 1K and 1L), although at a lower level than in immature TEs. These results indicate that

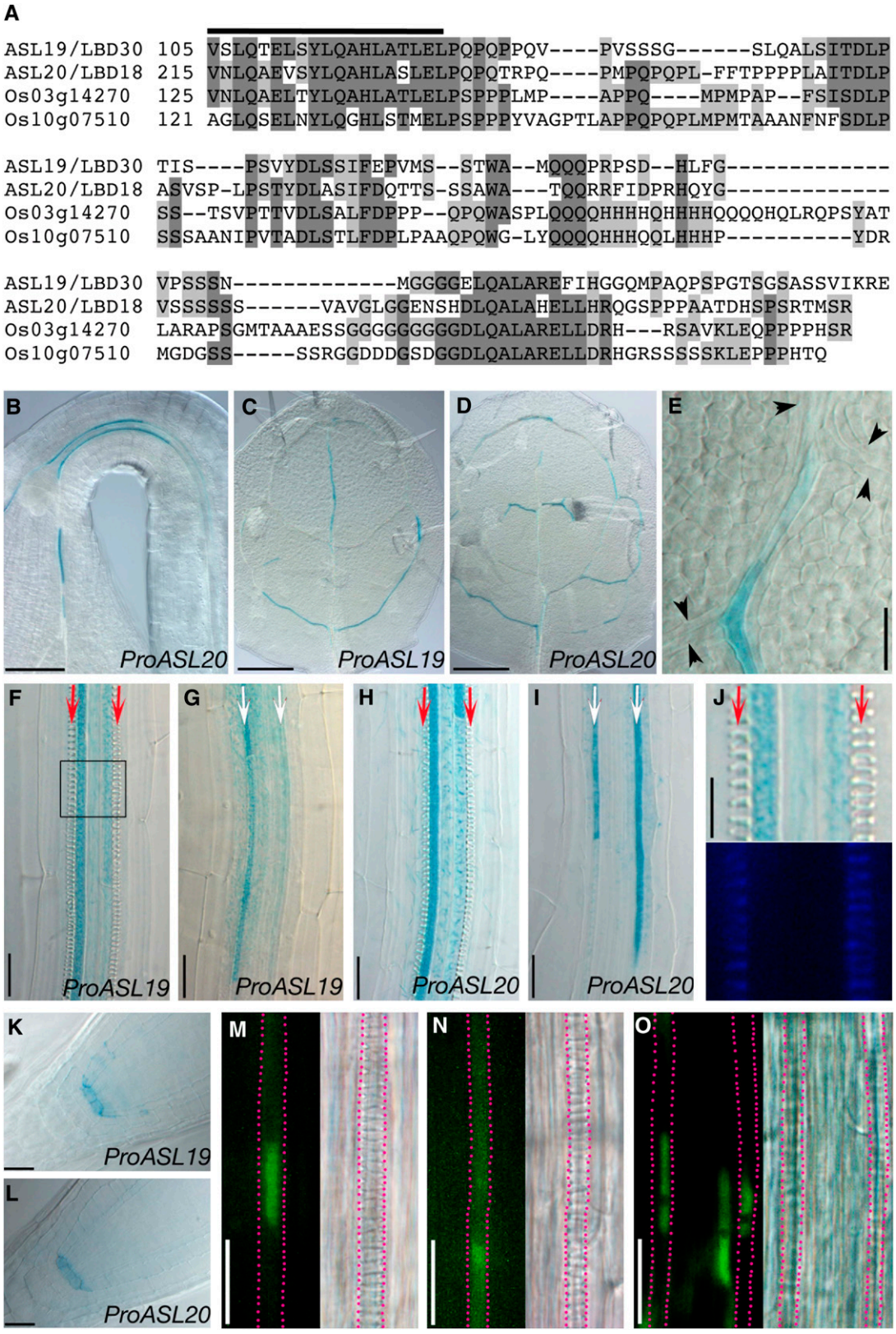

Figure 1. Similarity in Amino Acid Sequences of the C-Terminal Regions of *Arabidopsis* and Rice ASL Proteins, and Expression Patterns of *ASL19* and *ASL20*.

ASL19 and *ASL20* expression is closely associated with TE differentiation. The similar expression patterns of *ASL19* and *ASL20* are consistent with the hypothesis that these two genes have redundant functions.

Furthermore, we examined the subcellular localization of the ASL20-EGFP protein expressed from the native *ASL20* promoter. We detected most fluorescence in the nucleus and a faint signal in the cytoplasm of differentiating TEs (Figure 1M). This result was similar to the subcellular localization of EGFP appended with a nuclear localization signal from SV40 (Figure 1O). Green fluorescence from *ProASL20:EGFP-GUS* plants was detected throughout the cytoplasm (Figure 1N).

Overexpression of *ASL* Genes

To investigate the functions of ASL19 and ASL20 proteins, we overexpressed their corresponding cDNAs from a cauliflower mosaic virus *35S* promoter (*Pro35S*) or an estradiol-inducible system (XVE; for LexA-VP16-ER) (Zuo et al., 2000). *Pro35S:ASL19* and *Pro35S:ASL20* transgenic plants were dwarfed and produced short petioles and their leaves curled downward (Figures 2B and 2C). In addition, *Pro35S:ASL19* plants appeared bushy because of the generation of ectopic shoots (in 58% [*n* = 85] of T1 plants) (Figure 2B) from the adaxial side of cotyledons. The root tips of *Pro35S:ASL19* plants were shrunken, which inhibited root growth. Columella cells were also disorganized in *Pro35S:ASL20* plants. The root tip phenotype was similar to that reported for *jlo-D* (Borghi et al., 2007).

Overexpression of *ASL19* and *ASL20* from either a *35S* promoter or an XVE-inducible system did not influence the formation of xylem vessels. However, when transcription was induced by β-estradiol, multiple lines of *XVE:ASL19* and *XVE:ASL20* plants produced cells with wall thickenings, similar to those of protoxylem, in the mesophyll and epidermal tissues of cotyledons and in various tissues of the roots (Figures 2D to 2G and 2I). Similarly, *Pro35S:ASL20* lines formed TE-like cells in the cortex and stele of the roots (Figure 2J). UV illumination and staining with fuchsin showed lignin deposition in the wall thickenings of TE-like cells in cotyledons and of mature TEs (Figures 2D to 2G). Fluorescence emitted from chloroplasts in living mesophyll cells was not detectable in TE-like cells produced in the mesophyll tissues of *XVE:ASL20* plants (Figure 2G), suggesting that cell contents had been lost. TE-like cells in the roots were usually observed in the maturation region rather than in the apical region, which includes the differentiation zone. Generation of TE-like cells in plants overexpressing *ASL19* was less frequent than in those overexpressing *ASL20* (cf. Figures 2E and 2F). Control experiments showed that TE-like cells were not seen in plants overexpressing *ASL17*/*LBD14* and *ASL22*/*LBD31* (see Supplemental Figures 3C and 3D online), even though these plants were dwarfed and similar in morphology to plants overexpressing *ASL19* and *ASL20* (see Supplemental Figures 3A and 3B online). These results show that ASL19 and ASL20, but not ASL17 and ASL22, have the capacity to induce transdifferentiation of nonvascular cells into TE-like cells.

VND6 and *VND7* Regulated the Expression of *ASL* Genes

The overexpression of *VND6* or *VND7* produced TE-like cells from nonvascular tissues, similar to those formed when *ASL19* or *ASL20* was overexpressed (Kubo et al., 2005). We generated transgenic plants overexpressing *VND6* and *VND7* cDNAs using the inducible XVE system and performed real-time PCR to investigate the expression of *ASL19* and *ASL20* in these plants after treatment with β-estradiol. The levels of *ASL19* and *ASL20* mRNAs increased in both *XVE:VND6* and *XVE:VND7* plants within 8 h of β-estradiol treatment (Figure 3A). The expression of *XYN3*, encoding TE-specific xylanase (Sawa et al., 2005), was also induced. TE-like cells with deposited lignin appeared within 60 h of induction (Figure 3B). Induction of *ASL19* and *ASL20* expression preceded the appearance of visible TE-like cells. To investigate the effect of *VND6* and *VND7* on the expression pattern of *ASL19* and *ASL20*, we introduced *Pro35S:VND7* and *Pro35S:VND6* into plants carrying *ProASL19:EGFP-GUS* and *ProASL20:EGFP-GUS*. Histochemical GUS staining assays showed ectopic expression of both promoter–reporter genes in the nonvascular tissues of plants overexpressing *VND7* and *VND6* (Figure 3C). These results indicate that VND6 and VND7 operate upstream of *ASL19* and *ASL20*.

Since it has been reported that mutants of *VND6* and *VND7* do not exhibit significant phenotypes (Kubo et al., 2005), we constructed dominant-negative versions of VND6 and VND7 proteins by fusing with the SRDX artificial repression domain at their C termini (VND6-SRDX and VND7-SRDX) (Hiratsu et al., 2003; Kubo et al., 2005). We overexpressed cDNAs encoding these chimeric proteins using a *35S* promoter in *ProASL19:EGFP-GUS* and *ProASL20:EGFP-GUS* lines. The expression of *VND6-SRDX* and *VND7-SRDX* in transgenic plants affected the formation of

Figure 1. (continued).

(A) An alignment of amino acid sequences of *Arabidopsis* and rice ASL proteins. The thick line indicates the C-terminal ends of AS2/LOB domains.
(B) to **(L)** GUS staining in transgenic plants expressing *ProASL19:EGFP-GUS* (**[C]**, **[F]**, **[G]**, **[J]**, and [**K]**) and *ProASL20:EGFP-GUS* (**[B]**, **[D]**, **[E]**, **[H]**, **[I]**, and [**L]**). Apical hook of an etiolated seedling **(B)**, first or second leaf (**[C]** to [**E]**), maturation zones (**[F]**, **[H]**, and [**J]**; ~1.5 to 2 mm from root tips) and differentiation zones (**[G]** and **[I]**; ~0.4 to 0.8 mm from root tips) of roots and of root tips (**[K]** and **[L]**) of a seedling at 6 d after vernalization (DAV). **(J)** shows the boxed region in **(F)** at a higher magnification (top panel). Lignin deposited in protoxylem was visualized under UV illumination (bottom panel). Arrowheads in **(E)** indicate putative TE precursors. Note that putative TE precursors did not express *EGFP-GUS*. Arrows in **(F)** to **(I)** indicate cell files of protoxylem vessels with spiral wall thickenings (red) and undifferentiated TEs (white).
(M) to **(O)** Subcellular localization of the ASL20-EGFP protein. Fluorescence signals (left panels) due to ASL20-EGFP **(M)** and EGFP-GUS **(N)** driven by the *ASL20* promoter and due to EGFP-NLS **(O)** driven by a *35S* promoter and differential interference contrast images (right panels). Red dashed lines show immature TEs expressing EGFP fusion proteins.
Bars = 100 μm in **(B)** to **(D)**, 20 μm in **(E)** to **(I)**, **(K)**, and **(L)**, and 10 μm in **(J)** and **(M)** to **(O)**.

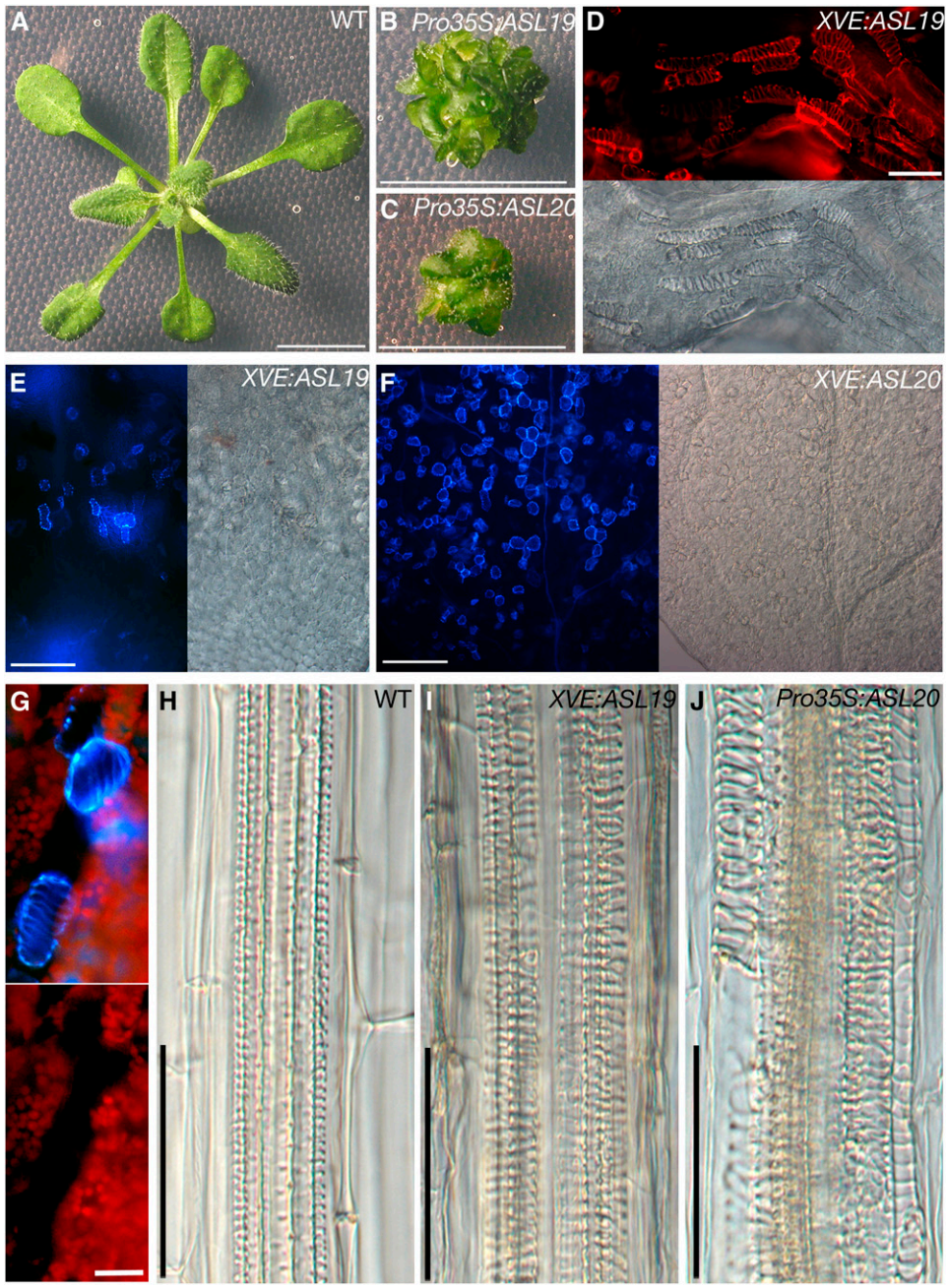

Figure 2. Ectopic Production of TE-Like Cells upon *ASL* Overexpression.

(A) to **(C)** Three-week-old seedlings of a wild-type plant **(A)**, a *Pro35S:ASL19* line **(B)**, and a *Pro35S:ASL20* line **(C)**.

(D) to **(J)** TE-like cells generated in seedlings (10 DAV) of *XVE:ASL19* (**[D]**, **[E]**, and **[I]**), *XVE:ASL20* (**[F]** and **[G]**), and *Pro35S:ASL20* **(J)** lines and wild-type control **(H)**. Seedlings (3 DAV) of *XVE:ASL19* and *XVE:ASL20* lines were transferred onto plates with 10 μM β-estradiol and grown for 7 d.

(D) Basal margin of a cotyledon and its petiole. Fluorescence image of TE-like cells stained with fuchsin (top panel) and the corresponding Nomarski image (bottom panel).

(E) and **(F)** Cotyledons. Fluorescence images of TE-like cells visualized by UV illumination (left panels) and the corresponding Nomarski images (right panels).

(G) Living mesophyll cells observed under UV illumination. Fluorescence from chloroplasts (red; top and bottom panels) and merged with an image showing lignin (blue; top panel).

(H) to **(J)** Nomarski images of roots.

Bars = 1 cm in **(A)** to **(C)**, 50 μm in **(D)** and **(H)** to **(J)**, 0.2 mm in **(E)** and **(F)**, and 20 μm in **(G)**.

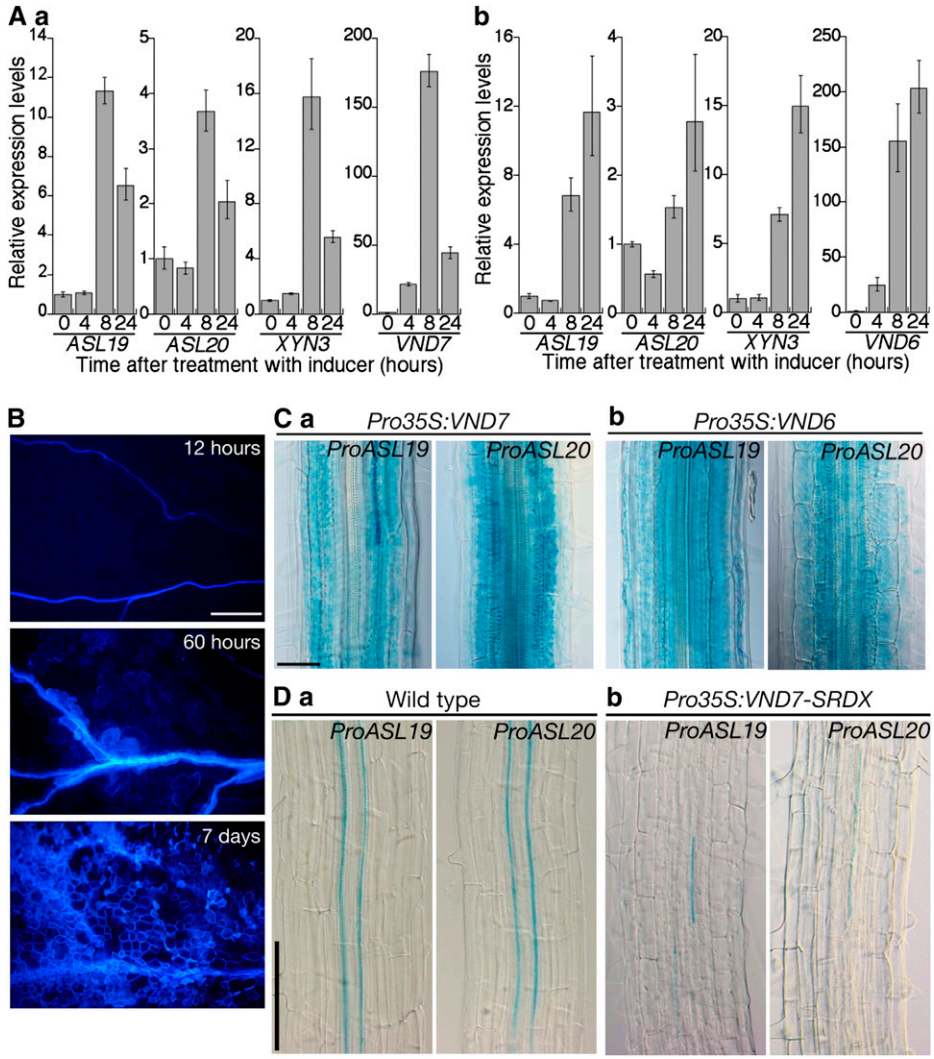

Figure 3. *VND6*- and *VND7*-Dependent Expression of *ASL19* and *ASL20*.

(A) Real-time PCR was performed with total RNA isolated from seedlings (10 DVA) of *XVE:VND7* **(a)** and *XVE:VND6* **(b)** lines that were incubated with 10 μM β-estradiol for the indicated times. Results are presented as averages of normalized relative transcript levels ± SD of three replicates.
(B) TE-like cells in cotyledons of *XVE:VND7* lines, as visualized under UV illumination. Seedlings (3 DAV) were treated with 10 μM β-estradiol for the indicated amounts of time.
(C) and **(D)** Expression of *ProASL19:EGFP-GUS* and *ProASL20:EGFP-GUS* in roots of *Pro35S:VND7* **(Ca)**, *Pro35S:VND6* **(Cb)**, and *Pro35S:VND7-SRDX* **(Db)** lines and in roots of control plants of the same age **(Da)**.
Bars = 200 μm in **(B)**, 50 μm in **(C)**, and 100 μm in **(D)**.

xylem vessels and produced discontinuous xylem vessels in the roots (Figure 3D; see Supplemental Figure 4A online) (Kubo et al., 2005). The expression of *ProASL19:EGFP-GUS* and *ProASL20:EGFP-GUS* was remarkably downregulated in these plants (Figure 3D; see Supplemental Figure 4A online). Weak and discontinuous GUS signals were observed in the cell files of protoxylem and metaxylem vessels. These results provide evidence that VND6 and VND7 are positive regulators of *ASL19* and *ASL20* expression and that their activities are required for ASL19/20 expression.

Since auxin and BR are required for the induction and progression of TE differentiation in an in vitro transdifferentiation system using isolated *Zinnia* mesophyll cells (Yamamoto et al., 1997; Fukuda, 2004), we also examined responses of *ASL19* and *ASL20* to these phytohormones. BR did not alter the expression of *ASL19* and *ASL20*, even at 12 h after treatment. By contrast, consistent with the results of the microarray analysis by Okushima et al. (2005), levels of *ASL20* mRNA, but not of *ASL19* mRNA, increased within 30 min of naphthylacetic acid treatment (see Supplemental Figure 5A online), and this increase was dependent on *AUXIN RESPONSE FACTOR7* (*ARF7*) (see Supplemental Figure 5B online). However, neither exogenous auxin nor the *arf7* mutation altered the expression pattern of *ProASL20:EGFP-GUS* (see Supplemental Figure 5C online). Our results indicate that auxin enhances the expression of *ASL20*.

Overexpression of *ASL20*-Induced Ectopic Expression of *VND7*

Since *ASL19* and *ASL20* expression in immature TE was dependent on VND6 and VND7 activities, we examined whether ASL19 and ASL20 proteins could rescue a deficiency in VND7 activity. To this end, we introduced *Pro35S:VND7-SRDX* into *XVE:ASL19* and *XVE:ASL20* transgenic lines. In the absence of β-estradiol, these transgenic plants showed defects in the differentiation of protoxylem vessels around the differentiation zone of roots (Figures 4A and 4C). In the presence of β-estradiol, the induced expression of *ASL19* and *ASL20* was confirmed by RT-PCR (see Supplemental Figure 6 online). *ASL19* and *ASL20* overexpression only partially rescued the defects of xylem vessel formation (Figures 4B and 4D to 4F). Similar results were also obtained in experiments using *Pro35S:VND6-SRDX* (see Supplemental Figure 4B online). These results indicate that the activities of VND6 and VND7 are required for ASL19 and ASL20 proteins to fully induce TE differentiation.

Next, we introduced *ProVND7:EGFP-GUS* into *XVE:ASL20* lines and performed a histochemical GUS staining assay. Note that the *VND7* promoter region fully includes the promoter used by Kubo et al. (2005). In the absence of β-estradiol, we detected GUS signals in immature TEs of both metaxylem and protoxylem vessels (Figure 4L; see Supplemental Figure 7 online), which is consistent with the recent result of Yamaguchi et al. (2008). GUS signals were not detected in the mesophyll and epidermal tissues of cotyledons (Figure 4G). In the presence of β-estradiol, the expression of *ProVND7:EGFP-GUS* was detected in the mesophyll and epidermal cells of cotyledons (Figure 4H) and in the nonvascular cells in the maturation region of roots (Figure 4K). We observed transdifferentiation of the mesophyll cells with GUS signals into TE-like cells (Figure 4I). Although ectopic *VND7* expression was not detected in the apical part of roots containing differentiating and immature TEs of protoxylem vessels, the intensity of GUS signals increased in immature TEs that were generated at developmentally normal positions (Figures 4L and 4M). Enhancement of *EGFP-GUS* expression in immature TEs was detected within 24 h of treatment. Ectopic expression of *ProVND7:EGFP-GUS* was detected from 3 d after inducer treatment.

To further confirm that *ASL19* and *ASL20* act downstream of *VND7*, we examined the metaxylem vessels of roots from plants transformed with promoter–*GUS* reporter constructs for *VND7*, *ASL19*, and *ASL20* and counted the number of TEs with GUS signals. There was no significant difference in the number of lignified TEs with GUS signals among plants expressing these three different reporter constructs (Figure 4O). By contrast, *ProVND7:EGFP-GUS* was expressed in more nonlignified TEs than were the other two reporter genes (Figure 4O). This result indicates that, in differentiating TEs, *VND7* expression occurs prior to that of *ASL19* and *ASL20*.

We assumed that the patchy pattern of *ProVND7:EGFP-GUS* expression (Figure 4H) might be due to the generation of specialized cells with procambial cell–like identity. To address this issue, we examined the expression of *ATHB-8*, a molecular marker for preprocambial and procambial cells (Baima et al., 1995; Scarpella et al., 2004), in *XVE:ASL20* plants using a *ProATHB-8:EGFP-GUS* reporter construct. Although GUS signals were detected in procambial cells along the vasculature of cotyledons, expression was not detected in the cells of other tissues, even when treated with β-estradiol (Figure 4N). This result suggests that the ectopic expression of *VND7* is not due to the generation of procambial cell–like cells.

ASL Activity Is Critical for Appropriate TE Differentiation

To investigate loss-of-function phenotypes of *ASL19* and *ASL20*, we obtained T-DNA and transposon insertion lines. The positions of T-DNA and transposon insertions are summarized in Supplemental Figure 1A online. RT-PCR analysis confirmed that these mutants are null, since *ASL19* and *ASL20* mRNAs were not detectable (see Supplemental Figure 1B online). Since the formation of xylem vessels was not significantly affected by *asl19-2* and *asl20-1* single mutations, we genetically created double mutants. However, double mutant plants did not exhibit any significant defect in xylem formation either.

We decided to use an alternative approach to investigate the loss-of-function phenotype. To this end, we constructed a cDNA encoding the ASL20 protein fused to the SRDX repressor domain at its C terminus (ASL20-SRDX). If the ASL20 protein acts on specific DNA sequences and positively regulates gene expression, the chimeric protein might downregulate gene expression downstream of *ASL20*. *ASL20-SRDX* cDNA was expressed from the native *ASL20* promoter.

We found that 50.4% (n = 107) of T1 transgenic plants were markedly smaller than wild-type plants (Figure 5A). Although venation patterns of cotyledons and leaves were not significantly altered (Figures 5B and 5C), we found abnormalities in the xylem vessels of dwarfed transgenic plants (Figures 5E, 5G, 5H, and 5J to 5L). Xylem vessels of midveins in the leaves of wild-type plants were tightly associated with each other. Each TE in the same xylem vessel was connected to its neighboring TEs (Figure 5D). In dwarf plants, by contrast, we observed extra spaces between the xylem vessels in midveins and found gaps between mature TEs (Figure 5E). In addition, leaves of dwarf plants formed TEs with pitted wall thickenings (Figures 5G and 5H), instead of the typical spiral wall thickenings seen in leaves of wild-type plants (Figure 5F). The pitted pattern of wall thickenings was similar to that of metaxylem (Figure 5I) and was not observed in leaves of wild-type plants. In roots of dwarfed plants, we also discovered abnormalities, including discontinuities of protoxylem vessels (Figures 5J and 5L), formation of TEs with pitted wall thickenings in cell files of protoxylem vessels (Figure 5K), and TEs with obscure wall thickenings (Figure 5L). Pitted patterns on wall thickenings of metaxylem vessels in dwarf plants were larger than those in wild-type plants (Figures 5I and 5K). We also observed delayed differentiation of metaxylem vessels in roots (see Supplemental Figures 8A to 8A′′ online) and isolated fragments of xylem vessels in cotyledons and leaves of dwarf plants (see Supplemental Figures 8C and 8D online). These results indicate that the ASL20-SRDX protein affects the formation of patterned secondary cell wall thickenings and partially inhibits TE differentiation.

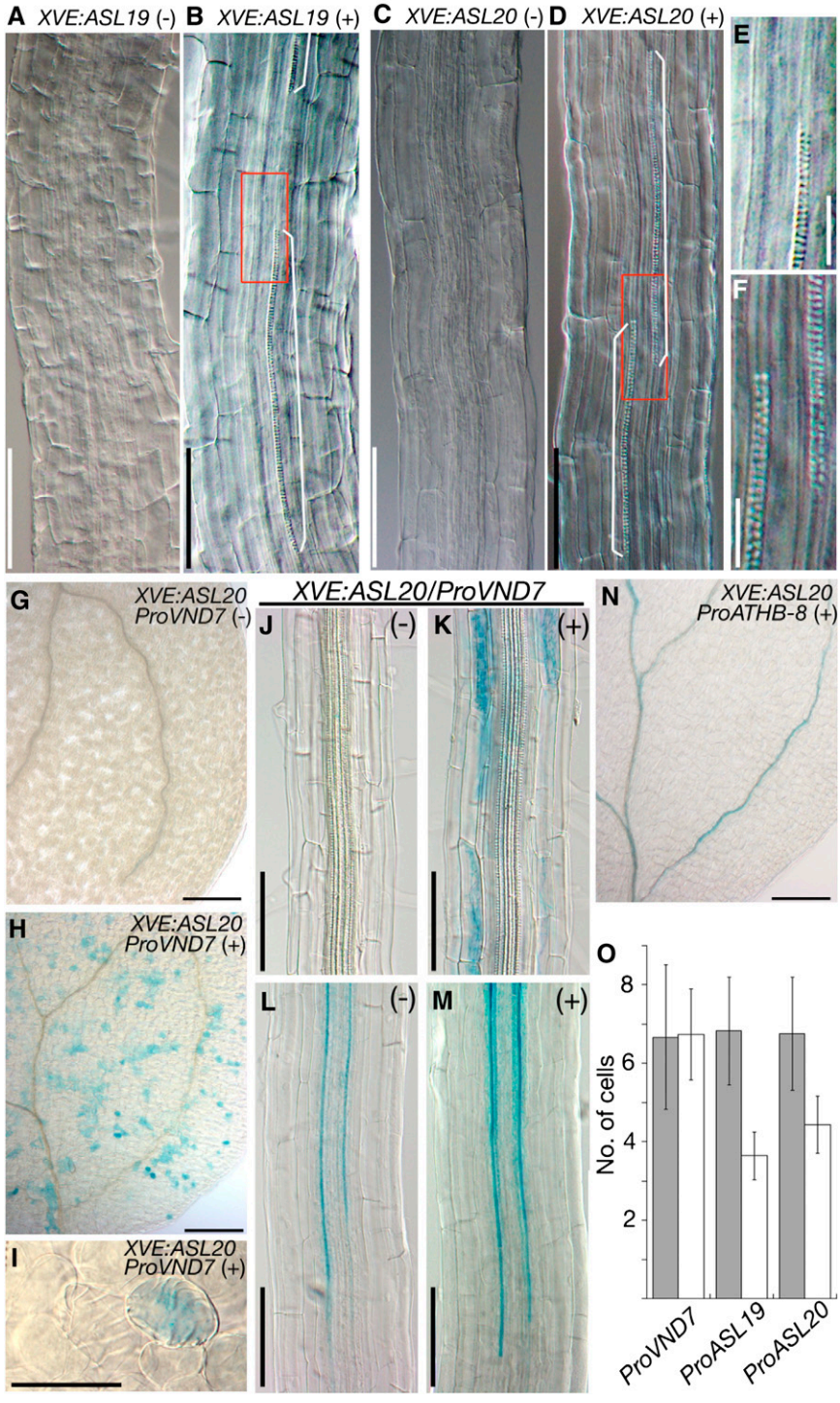

Figure 4. Overexpression of *ASL20* Induced Ectopic Expression of *VND7*.

(A) to **(F)** Roots of *Pro35S:VND7-SRDX* lines with either *XVE:ASL19* (**[A]** and **[B]**) or *XVE:ASL20* (**[C]** and **[D]**). Seedlings (3 DAV) were transferred onto plates with (+) or without (−) the inducer and grown for 4 d. White lines indicate fragments of protoxylem (**[B]** and **[D]**). Magnified images of the boxed regions in **(B)** and **(D)** are shown in **(E)** and **(F)**, respectively.

(G) to **(N)** GUS staining in cotyledons (**[G]** to **[I]** and **[N]**) and roots (**[J]** to **[M]**) of *XVE:ASL20* lines with *ProVND7:EGFP-GUS* (**[G]** to **[M]**) and *ProATHB-8:EGFP-GUS* **(N)**. Seedlings (3 DAV) were grown on plates with (+) or without (−) the inducer for 5 d. **(I)** shows a magnified image of a mesophyll cell with GUS staining transdifferentiating into TE-like cells. Maturation regions (**[J]** and **[K]**) and differentiation zones (**[L]** and **[M]**) of roots.

Effects of ASL20-SRDX on the Expression of Genes Related to TE Differentiation

We analyzed the effects of the ASL20-SRDX protein on the expression of *VND6* and *VND7* genes. Because dwarfed *ProASL20:ASL20-SRDX* transgenic lines died before bolting on soil, we separately collected T1 plants that exhibited the dwarf phenotype and transgenic plants that grew normally and prepared total RNA from these samples. Real-time PCR revealed that both *VND6* and *VND7* mRNA levels were reduced in dwarfed plants (Figure 6A). Reduced levels of mRNAs for endogenous *ASL19* and *ASL20* were also detected (Figure 6A). However, no significant difference in *ATHB-8* mRNA levels was detected between the two plant populations (Figure 6A). To further confirm *ASL20-SRDX* expression, we performed real-time PCR using a primer pair specific to the coding sequences for *SRDX*. We found that *ASL20-SRDX* mRNA accumulated to a higher level in this population than in plants with the wild-type phenotype (Figure 6A). Reduced levels of *VND7* expression in dwarfed *ProASL20:ASL20-SRDX* plants are consistent with the ectopic expression of *VND7* in plants overexpressing *ASL20*.

We further analyzed the expression of several TE differentiation-related genes, including *MAP65-8* (for MICROTUBULE-ASSOCIATED PROTEIN65 family protein), three secondary cell wall–related genes, *IRREGULAR XYLEM3* (*IRX3*)/*CesA7* (cellulose synthase) (Taylor et al., 1999), *IRX12* (laccase) (Brown et al., 2005; Sawa et al., 2005), and *XYN3* (xylanase) (Sawa et al., 2005), and a cell death–related gene, *XCP1* (for XYLEM CYS PROTEASE) (Funk et al., 2002). A microarray analysis (Kubo et al., 2005) previously showed that the expression of these genes is induced during transdifferentiation of *Arabidopsis* suspension culture cells into TEs, along with the induction of *ASL19*, *ASL20*, and *VND* genes. Of the genes encoding the *Arabidopsis* MAP65 family of proteins, *MAP65-8* was the only gene for which expression was upregulated in the *Arabidopsis* suspension culture cells after treatment to induce TE differentiation. We confirmed that the expression of these TE differentiation-related genes was induced by *VND7* overexpression (Figure 6B). By contrast, reduced expression of *MAP65-8*, *IRX3*, *IRX12*, *XYN3*, and *XCP1* was found in the population of dwarfed *ProASL20:ASL20-SRDX* lines (Figure 6A). These results show that the ASL20-SRDX protein downregulates the expression of genes related to TE differentiation, consistent with the downregulation of *VND6/7* expression by the ASL20-SRDX protein.

DISCUSSION

ASL19 and *ASL20* Positively Regulate TE Differentiation

Here, we investigated the function of *ASL19* and *ASL20* genes, which encode members of the *Arabidopsis* AS2/LBD family of proteins. Three lines of evidence implicate these two *ASL* genes in the regulation of TE differentiation. (1) Promoter analysis of *ASL19* and *ASL20* showed that they are specifically expressed in immature TEs (Figure 1). (2) The overexpression of *ASL19* and *ASL20* induced transdifferentiation of cells from nonvascular tissues into TE-like cells (Figure 2). (3) Aberrant TEs were formed when ASL20-SRDX, a dominant-negative version of ASL20, was expressed (Figure 5). Taken together, these results provide evidence that ASL proteins promote TE differentiation. Furthermore, similar expression patterns and the generation of TE-like cells by overexpression (Figures 1 and 2) support the notion that *ASL19* and *ASL20* function redundantly to regulate TE differentiation. By contrast, differences in phenotypic traits between plants overexpressing *ASL19* and *ASL20* (for instance, formation of ectopic shoots in *Pro35S:ASL19* plants and differences in efficiencies to induce TE-like cells; Figure 2) suggest that ASL19 and ASL20 have specific activities and actions as well.

Although double mutations in *ASL19* and *ASL20* did not affect the formation of xylem vessels, expression of ASL20-SRDX protein caused defects in TE differentiation (Figure 5; see Supplemental Figure 8 online). The partial inhibition of TE differentiation was an effect opposite to that seen when *ASL19/20* were overexpressed (Figures 2 and 5). These results suggest that the ASL20-SRDX protein dominantly interfered with the function of endogenous ASL proteins. A similar inhibitory effect of the repressor domain SRDX was also reported for the ASL18 protein (Okushima et al., 2007). With the exception of *as2*, mutants of *Arabidopsis AS2/LBD* family genes reported so far have not displayed any obvious phenotypes (Shuai et al., 2002; Nakazawa et al., 2003; Chalfun-Junior et al., 2005; Okushima et al., 2007). Transgenic plants overexpressing *ASL17*, *ASL19*, *ASL20*, and *ASL22* developed leaves with similar morphological alternations (Figures 2B and 2C; see Supplemental Figures 3A and 3B online), suggesting a high degree of functional redundancy among the AS2/LBD proteins. The effects of *asl19* and *asl20* mutations are most likely masked by functional redundancy. We used the native *ASL20* promoter to express *ASL20-SRDX* in plants. Among the several *AS2/LBD* genes tested, only *ASL19* and *ASL20* showed the capacity to induce the formation of TE-like cells (Figure 2; see Supplemental Figures 3C and 3D online). Therefore, the phenotype caused by ASL20-SRDX protein is most likely due to the inhibition of ASL proteins that redundantly function with ASL20.

ASL Genes Mediate a Feedback Pathway Downstream of *VND6* and *VND7*

VND6 and VND7 are key positive regulators of TE differentiation. The overexpression of these genes induces transdifferentiation of nonvascular cells into TE-like cells, similar to when *ASL19* and *ASL20* are overexpressed (Kubo et al., 2005). We demonstrated

Figure 4. (continued).

(O) Number of lignified (gray bars) and nonlignified (white bars) TEs with GUS signals in metaxylem vessels of roots. *ProVND7:EGFP-GUS* (*ProVND7*; n = 15), *ProASL19:EGFP-GUS* (*ProASL19*; n = 17), and *ProASL20:EGFP-GUS* (*ProASL20*; n = 16) lines (6 DAV). The error bars indicate SD.
Bars = 200 μm in **(A)** to **(D)** and **(J)** to **(M)**, 50 μm in **(E)** and **(F)**,100 μm in **(G)**, **(H)**, and **(N)**, and 20 μm in **(I)**.

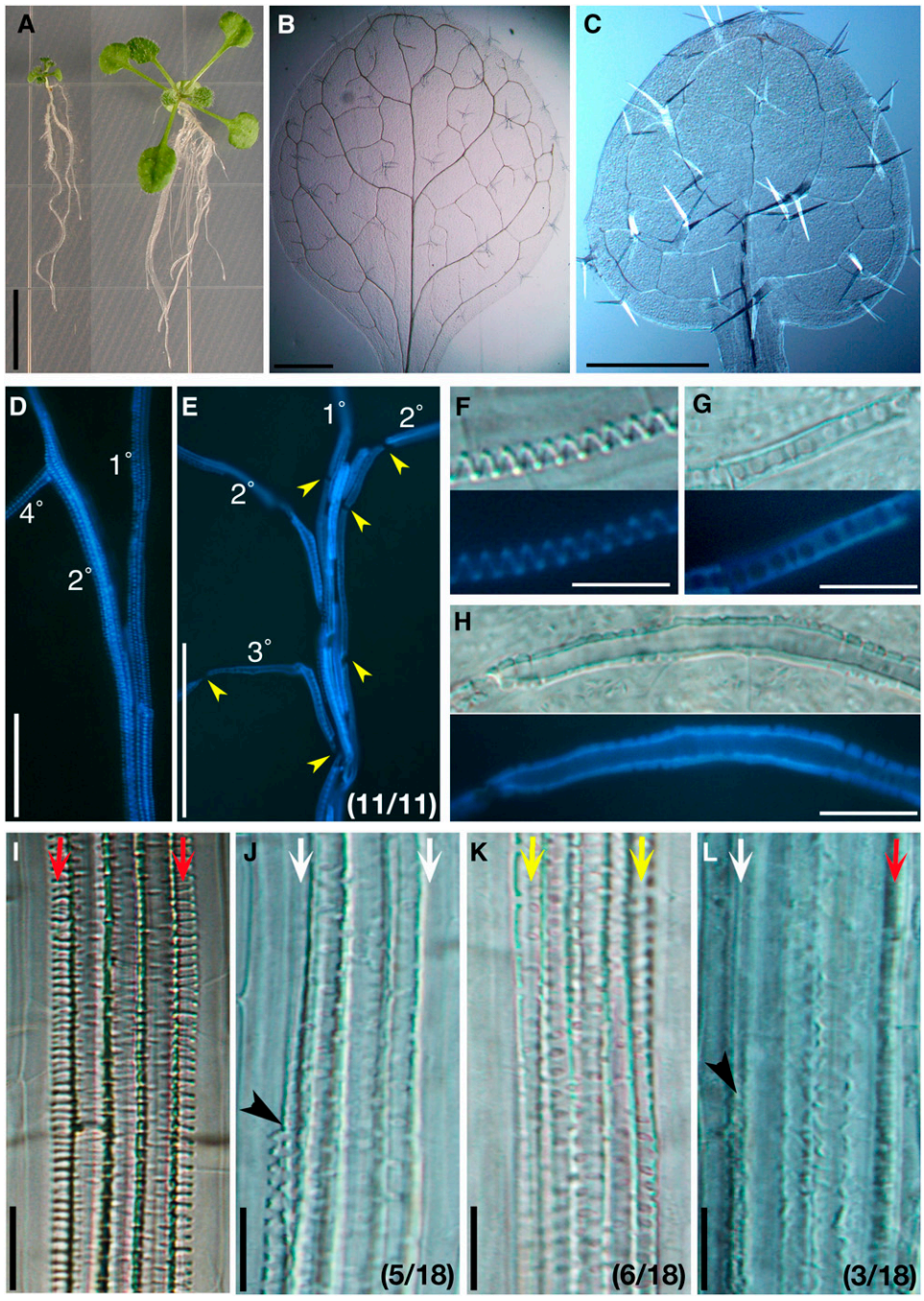

Figure 5. Phenotypic Analysis of *ProASL20:ASL20-SRDX* Plants.

(A) *ProASL20:ASL20-SRDX* plants (12 DAV) with the dwarf phenotype (left) and with normal growth (right).
(B) to **(H)** First leaf of wild-type (**[B]**, **[D]**, and **[F]**) and dwarfed *ProASL20:ASL20-SRDX* (**[C]**, **[E]**, **[G]**, and **[H]**) plants.
(B) and **(C)** Venation patterns.
(D) and **(E)** Xylem vessels of midveins, as visualized under UV illumination. Yellow arrowheads indicate gaps between TEs **(E)**. The fraction of dwarfed plants showing the indicated feature is in parentheses **(E)**.
(F) to **(H)** Magnified images of mature TEs. Nomarski images (top panels) and fluorescence images under UV illumination (bottom panels).
(I) to **(L)** Xylem vessels in roots of wild-type **(I)** and dwarfed *ProASL20:ASL20-SRDX* (**[J]** to **[L]**) plants. Arrows indicate cell files of protoxylem vessels with spiral wall thickenings (red), undifferentiated TEs (white), and TEs with pitted wall thickenings (yellow). Black arrowheads indicate discontinuities of protoxylem vessels. The fractions of plants showing the indicated features are in parentheses.
Bars = 1 cm in **(A)**, 1 mm in **(B)**, 0.5 mm in **(C)**, 0.1 mm in **(D)** and **(E)**, and 20 μm in **(F)** to **(L)**.

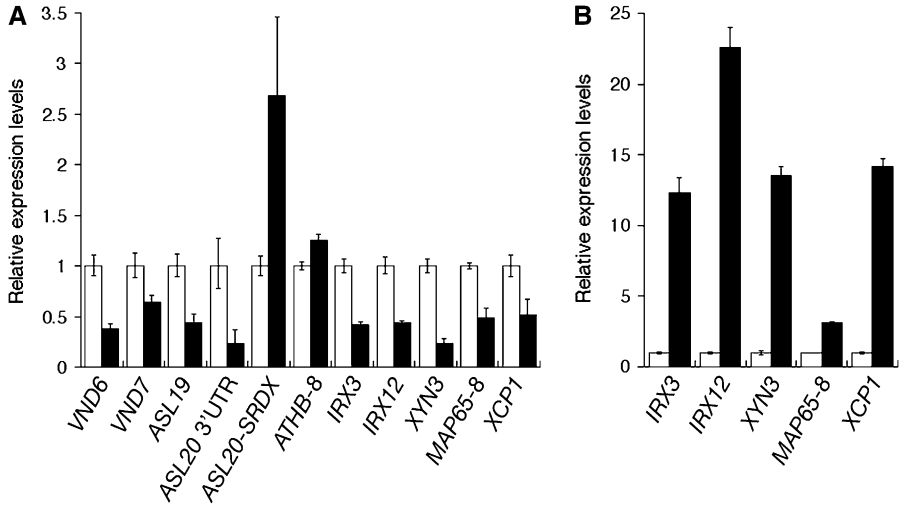

Figure 6. Effects of ASL20-SRDX on Expression of Genes Related to TE Differentiation.

(A) Expression of TE differentiation-related genes in *ProASL20:ASL20-SRDX* plants. Real-time PCR was performed with total RNA prepared from *ProASL20:ASL20-SRDX* lines showing the dwarf phenotype (closed bars) and normal growth (open bars). To detect the expression of the endogenous *ASL20* and that of *ASL20-SRDX*, primer pairs were used to amplify the 3′ untranslated region of *ASL20* (*ASL20* 3′UTR) and the coding sequence of SRDX, respectively. Results are presented as averages of normalized relative transcript levels ± SD of three technical replicates.

(B) Induction of TE differentiation-related genes by *VND7* overexpression. Real-time PCR was performed with total RNA prepared from *XVE:VND7* lines that were (closed bars) or were not (open bars) treated with 10 μM β-estradiol for 8 h. Results are presented as averages of normalized relative transcript levels ± SD of three technical replicates.

that VND6 and VND7 are positive regulators for *ASL19* and *ASL20* expression and are essential for *ASL19/20* expression in immature TEs (Figure 3). Therefore, we proposed that *ASL19* and *ASL20* act downstream of *VND6* and *VND7* in the regulation of TE differentiation. However, the xylem-deficient phenotype caused by the overexpression of dominant-negative versions of VND proteins was only partially rescued by *ASL19* and *ASL20* overexpression (Figures 4A to 4F; see Supplemental Figure 4B online). This observation raised three possibilities: (1) other factors under the regulation of VND6 and VND7 are required for the ASL19 and ASL20 proteins to fully function; (2) generation of ectopic TE-like cells by the overexpression of *ASL* genes is mediated by the expression of *VND6* and *VND7*; and (3) *ASL19* and *ASL20* are involved in only some events that occur during TE differentiation, such as biosynthesis of secondary cell wall compounds and their deposition. The third possibility appears unlikely, because we found loss of cell contents in TE-like cells (Figure 2G), suggesting the occurrence of autolysis, which is typical of the final step of TE differentiation; moreover, these TE-like cells displayed patterned formation of wall thickenings and lignin deposition. Ectopic expression of *VND7* in plants overexpressing *ASL20* (Figures 4H, 4I, and 4K) supported the second possibility, although the first possibility could not be excluded. Patchy patterns of *VND7* expression were similar to the distribution of TE-like cells produced in the cotyledon in response to *ASL20* overexpression (Figures 2F and 4H). Restriction of ectopic *VND7* expression to the mature region of the root also corresponded to the root region where TE-like cells were generated due to *ASL20* overexpression (Figures 2J, 4K, and 4M). Since *ASL20* overexpression did not alter the expression pattern of *ATHB-8* (Figure 4N), *ASL20* probably affected *VND7* expression and generated TE-like cells without acquiring procambial cell–like identity. Considering that VND6 and VND7 are required for the expression of *ASL19* and *ASL20* and that *VND7* expression occurs prior to that of *ASL19/20* genes in immature TEs, it is possible that *ASL19/20* genes are involved in a positive-feedback loop for *VND7* expression (Figure 7). This proposal is also consistent with the reduced levels of *VND6* and *VND7* mRNAs found in plants expressing *ProASL20:ASL20-SRDX* (Figure 6A).

Kubo et al. (2005) reported that T-DNA insertion mutants and expression of RNA interference constructs for *VND6* and *VND7*

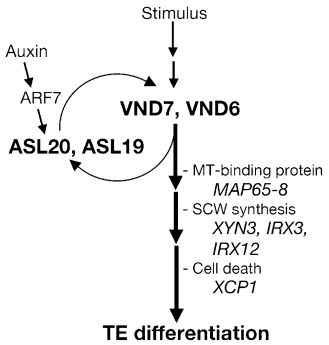

Figure 7. A Model Showing the Feedback Pathway Mediated by *ASL19* and *ASL20* to Maintain *VND6/7* Expression during TE Differentiation.

SCW, secondary cell wall.

did not yield any detectable defects in plant morphology, presumably due to gene function redundancy. However, the ASL20-SRDX protein interfered with the formation of TEs even if the expression of *VND6* and *VND7* was not completely repressed (Figures 5 and 6A). These results suggest that ASL20 regulates the expression of other genes involved in TE differentiation as well as *VND6* and *VND7*. This notion is consistent with the partial suppression of the xylem-deficient phenotype of *Pro35S:VND7-SRDX* plants by *ASL19* and *ASL20* overexpression. Yamaguchi et al. (2008) reported that expression domains of *VND* genes, including *VND6* and *VND7*, partially overlapped and that VND7 interacted with other VND proteins. ASL19 and ASL20 may also regulate the expression of *VND* genes other than *VND6* and *VND7*.

ASL20 Activity Is Required for Proper Development of Xylem Vessels

Plants expressing ASL20-SRDX protein from the *ASL20* promoter were affected in several aspects of xylem vessel formation. We detected loose bundling of xylem vessels in the leaves of these plants, physical gaps between mature TEs in the same cell file, aberrant patterns of wall thickenings, and delayed formation and discontinuities of xylem vessels (Figures 5D to 5L). Formation of gaps between mature TEs and loose bundling of xylem vessels in the leaves were probably due to the reduced flexibility of pitted wall thickenings being unable to withstand the forces of stretching that occur during organ expansion. *Arabidopsis* mutants with discontinuities of xylem vessels are often dwarfed, similar to *ProASL20:ASL20-SRDX* plants (Turner et al., 2007). No alteration in the vascular patterns in the leaves or in the levels of *ATHB-8* mRNA in transgenic plants indicates that ASL20-SRDX did not affect the formation of procambial cells (Figures 5C and 6A). Therefore, the delayed formation of wall thickenings and discontinuities of xylem vessels were due to a partial inhibition of TE differentiation by the ASL20-SRDX protein. Similar defects in TE differentiation were also observed in plants expressing dominant-negative versions of VND6 and VND7 proteins (Kubo et al., 2005).

Differentiation of TEs is a complex cellular process that is both temporally and spatially coordinated. This process includes cell expansion, rearrangement of cortical microtubules (MTs), secondary cell wall biosynthesis and deposition, and autolysis. Any changes in this series of events will result in the formation of inappropriate patterns of wall thickenings. Therefore, a positive feedback mechanism that could account for the expression of genes related to TE differentiation would be important to orchestrate this highly organized process. The sites for deposition of cellulose and other secondary cell wall compounds have been thought to be marked by bundles of cortical MTs, which are reorganized in developing TEs before and during the formation of secondary cell wall thickenings (Hogetsu, 1991; Gardiner et al., 2003; Oda et al., 2005). Interestingly, the formation of different types of wall thickenings by the overexpression of *VND6* and *VND7* suggests that they regulate the expression of genes involved in the reorganization of cortical MTs during TE differentiation. Furthermore, we showed that overexpression of the ASL20-SRDX protein resulted in the downregulation of *MAP65-8* together with genes related to secondary cell wall formation and to autolysis in dwarf *ProASL20:ASL20-SRDX* transgenic lines (Figure 6A). MAP65 proteins are known to bundle MTs and localize to cortical MTs during TE differentiation (Mao et al., 2006). Expression of these TE differentiation–related genes was also induced by *VND7* overexpression (Figure 6B). This result suggests that the ASL20-SRDX protein interferes with the expression of *MAP65-8*, *IRX3*, *IRX12*, *XYN3*, and *XCP1* through the downregulation of *VND6* and *VND7*, which leads to the formation of aberrant patterns of wall thickenings and the partial inhibition of TE differentiation. ASL19 and ASL20 may coordinate and stabilize gene expression status during the irreversible process of TE differentiation by maintaining or promoting *VND6*/*VND7* expression (Figure 7).

The inhibitory effects of ASL20-SRDX on TE differentiation (Figures 5 and 6) suggest that ASL20 functions on specific DNA sequences to positively regulate gene expression. *VND6* and *VND7* are possible candidates for genes targeted by ASL19/20 proteins. However, the overexpression of *VND6* and *VND7* more efficiently generated TE-like cells than the overexpression of *ASL19* and *ASL20* (cf. Figures 2E and 2F with Figure 3B). Furthermore, ectopic expression of *VND7* was detectable 3 d after the induction of *ASL20* overexpression. By contrast, enhancement of *VND7* expression in immature TEs was detected within 24 h of induction of *ASL20* overexpression. These results suggest that additional factors are required for ASL proteins to induce transcription of *VND6* and *VND7*. Identifying the components in protein complexes containing ASL19/20 is important to further elucidate the molecular functions of the ASL19 and ASL20 proteins.

METHODS

Plant Materials and Growth Conditions

Arabidopsis thaliana (ecotype Columbia) was used as the wild type. Plants were germinated on sterile Murashige and Skoog medium (0.8% agar) at 23°C under continuous light conditions after vernalization treatment (at 4°C in the dark for 2 d). Fourteen days after vernalization (DAV), plants grown on plates were transferred to soil and further grown in a greenhouse at 25°C with a photoperiod of 16 h of light and 8 h of darkness. *Agrobacterium tumefaciens*–mediated genetic transformation of *Arabidopsis* was done by the floral dip method (Clough and Bent, 1998).

Construction of Plasmids

cDNAs for *ASL19*, *ASL20*, *VND6*, and *VND7* and promoter regions of *ASL19* (2055 bp), *ASL20* (2082 bp), *VND7* (2000 bp), and *ATHB-8* (2004 bp) were amplified from cDNA pools as well as from genomic DNA using PCR with specific primer pairs (see Supplemental Table 1 online). cDNA fragments for each gene and DNA fragments for the promoter regions of *VND7* and *ATHB-8* were digested at sites present in the linker sequences with restriction enzymes, and the resulting fragments were ligated into an entry vector, pENTR-1A (Invitrogen). Promoter regions of *ASL19* and *ASL20* were cloned into the pCR8/GW/TOPO vector (Invitrogen) and into the pGEM-T Easy vector (Promega), respectively. An *Ava*I-*Not*I fragment containing the *ASL20* promoter in pGEM-T was inserted into pENTR-1A using *Sal*I and *Not*I sites. A coding sequence for SRDX was translationally fused to the 3′ end of *VND7* cDNA in pENTR-1A by PCR. The *VND7* cDNA

fragment of *VND7-SRDX* was replaced by *VND6* and *ASL20* cDNAs to generate *VND6-SRDX* and *ASL20-SRDX*. A translational fusion of *ASL20* and *EGFP* was generated by the insertion of the *EGFP* coding sequence at the 3′ end of *ASL20* cDNA from which the stop codon was removed in pENTR-1A. For *ProASL20:ASL20-EGFP* and *ProASL20:ASL20-SRDX*, fragments of *ASL20-EGFP* and *ASL20-SRDX* were inserted downstream of the *ASL20* promoter in pENTR-1A, using *Eco*RI and *Xho*I sites. Promoter fragments and cDNAs in entry vectors were transferred into destination vectors pKGWFS7, pB2GW7 (Karimi et al., 2002), and pER8-DC by LR clonase (Invitrogen). *ProASL20:ASL20-EGFP* and *ProASL20:ASL20-SRDX* were transferred into pBA-DC-HA from which the cauliflower mosaic virus 35S promoter was removed.

Histochemical GUS Staining Assay

Transgenic plants were treated with 90% acetone for 20 min at 4°C, washed three times with 100 mM $NaPO_4$ buffer (pH 7.0), and incubated with a staining solution [100 mM $NaPO_4$ (pH 7.0), 10 mM EDTA, 0.5 mg/mL 5-bromo-4-chloro-3-indolyl-β-glucuronic acid (LabScientific), 3 mM $K_4Fe(CN)_6$, 3 mM $K_3Fe(CN)_6$, and 0.1% Triton X-100] for 45 min to 2 h at 37°C. Samples were then incubated in acetic acid:ethanol (1:6) to fix the tissues and to remove chlorophyll.

Real-Time PCR

Total RNA was prepared with the RNeasy Plant Mini Kit (Qiagen) and the RNase-Free DNase Set (Qiagen). cDNA synthesis was performed using oligo$(dT)_{20}$ primer (Invitrogen) and Ready-to-Go You Prime First-Strand Synthesis Beads (GE Healthcare). Real-time PCR was performed with the 7100 real-time PCR system and Power SYBER Green PCR Master Mix (AB) as described in the manufacturer's protocols. Sequences of primers used for real-time PCR are presented in Supplemental Table 1 online. Relative amounts of PCR products were calculated with the ΔΔCt method, with DNA fragments amplified with a primer pair specific to α-*tubulin* cDNA serving as an internal control.

Microscopic Analysis

Plant samples were fixed with acetic acid:ethanol (1:6) for 1 h or overnight. The fixed samples were serially treated with 70% ethanol, 35% ethanol, and 10% ethanol for 30 min. Staining of TE-like cells with fuchsin was performed according to Mähönen et al. (2006). Samples were mounted on a clearing solution (8 g of chloral hydrate, 1 mL of glycerol, and 2 mL of water) before observation. Images of leaf venation patterns were captured using a stereoscopic microscope (SMZ-U; Nikon) equipped with a digital camera (COOLPIX5400; Nikon). Fluorescence and Nomarski images were captured using Axioskop (Carl Zeiss) equipped with a HBO100 microscope illuminator (Carl Zeiss) and a cooled CCD camera system (Diagnostic Instruments).

Accession Numbers

Sequence data from this article can be found in the Arabidopsis Genome Initiative databases under the following accession numbers: *ATHB-8* (At4g32880), *ASL19* (At4g00220), *ASL20* (Atg45420), *IRX3* (At5g17427), *IRX12* (At2g38030), *MAP65-8* (At1g27920), *VND6* (At5g62380), *VND7* (At1g71930), *XCP1* (At4g35350), and *XYN3* (At4g08160).

Supplemental Data

The following materials are available in the online version of this article.

Supplemental Figure 1. Mutations in *ASL19* and *ASL20.*

Supplemental Figure 2. Expression of *ProASL20:EGFP-GUS* and *ProASL19:EGFP-GUS* in Floral Organs and Siliques.

Supplemental Figure 3. Overexpression of *ASL17* and *ASL22* cDNAs.

Supplemental Figure 4. Overexpression of *VND6-SRDX*.

Supplemental Figure 5. Enhancement of *ASL20* Expression by Auxin.

Supplemental Figure 6. Expression of *ASL19* and *ASL20* in *XVE-ASL19 Pro35S:VND7-SRDX* Plants and *XVE-ASL20 Pro35S:VND7-SRDX* Plants.

Supplemental Figure 7. GUS Staining in Transgenic Plants Expressing *ProVND7:EGFP-GUS*.

Supplemental Figure 8. Delayed Formation and Discontinuities of Xylem Vessels.

Supplemental Table 1. Sequences of Primers.

ACKNOWLEDGMENTS

We thank the Cold Spring Harbor Laboratory and the ABRC for providing seeds. We thank Yoshihisa Ueno (Nagoya University) and Rossana Henriques (The Rockefeller University) for critical reading of the manuscript and discussion. T.S. was supported by a fellowship from the Human Frontier Science Program Organization (Grant LT00194/2005-L/5). This work was supported by National Institutes of Health Grant GM-44640 to N.-H.C.

Received June 29, 2008; revised November 20, 2008; accepted December 2, 2008; published December 16, 2008.

REFERENCES

Baima, S., Nobili, F., Sessa, G., Lucchetti, S., Ruberti, I., and Morelli, G. (1995). The expression of the *Athb-8* homeobox gene is restricted to provascular cells in *Arabidopsis thaliana*. Development **121:** 4171–4182.

Borghi, L., Bureau, M., and Simon, R. (2007). *Arabidopsis JAGGED LATERAL ORGANS* is expressed in boundaries and coordinates KNOX and PIN activity. Plant Cell **19:** 1795–1808.

Bortiri, E., Chuck, G., Vollbrecht, E., Rocheford, T., Martienssen, R., and Hake, S. (2006). *ramosa2* encodes a LATERAL ORGAN BOUNDARY domain protein that determines the fate of stem cells in branch meristems of maize. Plant Cell **18:** 574–585.

Brown, D.M., Zeef, L.A., Ellis, J., Goodacre, R., and Turner, S.R. (2005). Identification of novel genes in *Arabidopsis* involved in secondary cell wall formation using expression profiling and reverse genetics. Plant Cell **17:** 2281–2295.

Caño-Delgado, A., Yin, Y., Yu, C., Vafeados, D., Mora-Garcia, S., Cheng, J.C., Nam, K.H., Li, J., and Chory, J. (2004). *BRL1* and *BRL3* are novel brassinosteroid receptors that function in vascular differentiation in *Arabidopsis*. Development **131:** 5341–5351.

Chalfun-Junior, A., Franken, J., Mes, J.J., Marsch-Martinez, N., Pereira, A., and Angenent, G.C. (2005). *ASYMMETRIC LEAVES2-LIKE1* gene, a member of the AS2/LOB family, controls proximal–distal patterning in *Arabidopsis* petals. Plant Mol. Biol. **57:** 559–575.

Choe, S., Dilkes, B.P., Gregory, B.D., Ross, A.S., Yuan, H., Noguchi, T., Fujioka, S., Takatsuto, S., Tanaka, A., Yoshida, S., Tax, F.E., and Feldmann, K.A. (1999). The Arabidopsis *dwarf1* mutant is defective in the conversion of 24-methylenecholesterol to campesterol in brassinosteroid biosynthesis. Plant Physiol. **119:** 897–907.

Clough, S.J., and Bent, A.F. (1998). Floral dip: A simplified method for *Agrobacterium*-mediated transformation of *Arabidopsis thaliana*. Plant J. **16:** 735–743.

Evans, M.M. (2007). The indeterminate gametophyte1 gene of maize encodes a LOB domain protein required for embryo sac and leaf development. Plant Cell **19:** 46–62.

Fukuda, H. (2004). Signals that control plant vascular cell differentiation. Nat. Rev. Mol. Cell Biol. **5:** 379–391.

Funk, V., Kositsup, B., Zhao, C., and Beers, E.P. (2002). The Arabidopsis xylem peptidase XCP1 is a tracheary element vacuolar protein that may be a papain ortholog. Plant Physiol. **128:** 84–94.

Gardiner, J.C., Taylor, N.G., and Turner, S.R. (2003). Control of cellulose synthase complex localization in developing xylem. Plant Cell **15:** 1740–1748.

Guo, M., Thomas, J., Collins, G., and Timmermansa, M.C.P. (2008). Direct repression of *KNOX* loci by the ASYMMETRIC LEAVES1 complex of *Arabidopsis*. Plant Cell **20:** 48–58.

Hiratsu, K., Matsui, K., Koyama, T., and Ohme-Takagi, M. (2003). Dominant repression of target genes by chimeric repressors that include the EAR motif, a repression domain, in *Arabidopsis*. Plant J. **34:** 733–739.

Hogetsu, T. (1991). Mechanism for formation of the secondary wall thickening in tracheary elements—Microtubules and microfibrils of tracheary elements of *Pisum sativum* L and *Commelina communis* L and the effects of amiprophosmethyl. Planta **185:** 190–200.

Husbands, A., Bell, E.M., Shuai, B., Smith, H.M., and Springer, P.S. (2007). LATERAL ORGAN BOUNDARIES defines a new family of DNA-binding transcription factors and can interact with specific bHLH proteins. Nucleic Acids Res. **35:** 6663–6671.

Inukai, Y., Sakamoto, T., Ueguchi-Tanaka, M., Shibata, Y., Gomi, K., Umemura, I., Hasegawa, Y., Ashikari, M., Kitano, H., and Matsuoka, M. (2005). *Crown rootless1*, which is essential for crown root formation in rice, is a target of an AUXIN RESPONSE FACTOR in auxin signaling. Plant Cell **17:** 1387–1396.

Ito, Y., Nakanomyo, I., Motose, H., Iwamoto, K., Sawa, S., Dohmae, N., and Fukuda, H. (2006). Dodeca-CLE peptides as suppressors of plant stem cell differentiation. Science **313:** 842–845.

Iwakawa, H., Ueno, Y., Semiarti, E., Onouchi, H., Kojima, S., Tsukaya, H., Hasebe, M., Soma, T., Ikezaki, M., Machida, C., and Machida, Y. (2002). The *ASYMMETRIC LEAVES2* gene of *Arabidopsis thaliana*, required for formation of a symmetric flat leaf lamina, encodes a member of a novel family of proteins characterized by cysteine repeats and a leucine zipper. Plant Cell Physiol. **43:** 467–478.

Karimi, M., Inze, D., and Depicker, A. (2002). Gateway vectors for *Agrobacterium*-mediated plant transformation. Trends Plant Sci. **7:** 193–195.

Kubo, M., Udagawa, M., Nishikubo, N., Horiguchi, G., Yamaguchi, M., Ito, J., Mimura, T., Fukuda, H., and Demura, T. (2005). Transcription switches for protoxylem and metaxylem vessel formation. Genes Dev. **19:** 1855–1860.

Lin, W.C., Shuai, B., and Springer, P.S. (2003). The Arabidopsis *LATERAL ORGAN BOUNDARIES*-domain gene *ASYMMETRIC LEAVES2* functions in the repression of *KNOX* gene expression and in adaxial-abaxial patterning. Plant Cell **15:** 2241–2252.

Lincoln, C., Long, J., Yamaguchi, J., Serikawa, K., and Hake, S. (1994). A *knotted1-like homeobox* gene in *Arabidopsis* is expressed in the vegetative meristem and dramatically alters leaf morphology when overexpressed in transgenic plants. Plant Cell **12:** 1859–1876.

Liu, H., Wang, S., Yu, X., Yu, J., He, X., Zhang, S., Shou, H., and Wu, P. (2005). ARL1, a LOB-domain protein required for adventitious root formation in rice. Plant J. **43:** 47–56.

Mähönen, A.P., Bishopp, A., Higuchi, M., Nieminen, K.M., Kinoshita, K., Törmäkangas, K., Ikeda, Y., Oka, A., Kakimoto, T., and Helariutta, Y. (2006). Cytokinin signaling and its inhibitor AHP6 regulate cell fate during vascular development. Science **311:** 94–98.

Mao, G., Buschmann, H., Doonan, J.H., and Lloyd, C.W. (2006). The role of MAP65-1 in microtubule bundling during *Zinnia* tracheary element formation. J. Cell Sci. **119:** 753–758.

Motose, H., Sugiyama, M., and Fukuda, H. (2004). A proteoglycan mediates inductive interaction during plant vascular development. Nature **429:** 873–878.

Naito, T., Yamashino, T., Kiba, T., Koizumi, N., Kojima, M., Sakakibara, H., and Mizuno, T. (2007). A link between cytokinin and *ASL9* (*ASYMMETRIC LEAVES 2 LIKE 9*) that belongs to the *AS2*/*LOB* (*LATERAL ORGAN BOUNDARIES*) family genes in *Arabidopsis thaliana*. Biosci. Biotechnol. Biochem. **71:** 1269–1278.

Nakazawa, M., Ichikawa, T., Ishikawa, A., Kobayashi, H., Tsuhara, Y., Kawashima, M., Suzuki, K., Muto, S., and Matsui, M. (2003). Activation tagging, a novel tool to dissect the functions of a gene family. Plant J. **34:** 741–750.

Oda, Y., Mimura, T., and Hasezawa, S. (2005). Regulation of secondary cell wall development by cortical microtubules during tracheary element differentiation in *Arabidopsis* cell suspensions. Plant Physiol. **137:** 1027–1036.

Okushima, Y., Fukaki, H., Onoda, M., Theologis, A., and Tasaka, M. (2007). ARF7 and ARF19 regulate lateral root formation via direct activation of *LBD*/*ASL* genes in *Arabidopsis*. Plant Cell **19:** 118–130.

Okushima, Y., et al. (2005). Functional genomic analysis of the *AUXIN RESPONSE FACTOR* gene family members in *Arabidopsis thaliana*: Unique and overlapping functions of *ARF7* and *ARF19*. Plant Cell **17:** 444–463.

Ori, N., Eshed, Y., Chuck, G., Bowman, J.L., and Hake, S. (2000). Mechanisms that control knox gene expression in the *Arabidopsis* shoot. Development **127:** 5523–5532.

Pyo, H., Demura, T., and Fukuda, H. (2004). Spatial and temporal tracing of vessel differentiation in young *Arabidopsis* seedlings by the expression of an immature tracheary element-specific promoter. Plant Cell Physiol. **45:** 1529–1536.

Sawa, S., Demura, T., Horiguchi, G., Kubo, M., and Fukuda, H. (2005). The *ATE* genes are responsible for repression of transdifferentiation into xylem cells in Arabidopsis. Plant Physiol. **137:** 141–148.

Scarpella, E., Francis, P., and Berleth, T. (2004). Stage-specific markers define early steps of procambium development in *Arabidopsis* leaves and correlate termination of vein formation with mesophyll differentiation. Development **131:** 3445–3455.

Semiarti, E., Ueno, Y., Tsukaya, H., Iwakawa, H., Machida, C., and Machida, Y. (2001). The *ASYMMETRIC LEAVES2* gene of *Arabidopsis thaliana* regulates formation of a symmetric lamina, establishment of venation and repression of meristem-related homeobox genes in leaves. Development **128:** 1771–1783.

Shuai, B., Reynaga-Pena, C.G., and Springer, P.S. (2002). The *LATERAL ORGANBOUNDARIES* gene defines a novel, plant-specific gene family. Plant Physiol. **129:** 747–761.

Szekeres, M., Nemeth, K., Koncz-Kalman, Z., Mathur, J., Kauschmann, A., Altmann, T., Redei, G.P., Nagy, F., Schell, J., and Koncz, C. (1996). Brassinosteroids rescue the deficiency of CYP90, a cytochrome P450, controlling cell elongation and de-etiolation in Arabidopsis. Cell **85:** 171–182.

Taramino, G., Sauer, M., Stauffer, J.L., Jr., Multani, D., Niu, X., Sakai, H., and Hochholdinger, F. (2007). The maize (*Zea mays* L.) *RTCS* gene encodes a LOB domain protein that is a key regulator of embryonic seminal and post-embryonic shoot-borne root initiation. Plant J. **50:** 649–659.

Taylor, N.G., Scheible, W.R., Cutler, S., Somerville, C.R., and Turner,

S.R. (1999). The *irregular xylem3* locus of Arabidopsis encodes a cellulose synthase required for secondary cell wall synthesis. Plant Cell **11:** 769–780.

Turner, S., Gallois, P., and Brown, D. (2007). Tracheary element differentiation. Annu. Rev. Plant Biol. **58:** 407–433.

Xu, L., Xu, Y., Dong, A., Sun, Y., Pi, L., Xu, Y., and Huang, H. (2003). Novel *as1* and *as2* defects in leaf adaxial-abaxial polarity reveal the requirement for *ASYMMETRIC LEAVES1* and *2* and *ERECTA* functions in specifying leaf adaxial identity. Development **130:** 4097–4107.

Yamaguchi, M., Kubo, M., Fukuda, H., and Demura, T. (2008). VASCULAR-RELATED NAC-DOMAIN7 is involved in differentiation of all types of xylem vessels in Arabidopsis roots and shoots. Plant J. **55:** 652–664.

Yamamoto, R., Demura, T., and Fukuda, H. (1997). Brassinosteroids induce entry into the final stage of tracheary element differentiation in cultured *Zinnia* cells. Plant Cell Physiol. **38:** 980–983.

Zuo, J., Niu, Q.W., and Chua, N.-H. (2000). An estrogen receptor-based transactivator XVE mediates highly inducible gene expression in transgenic plants. Plant J. **24:** 265–273.